

is the section area, or  $N$  is the number of intercepts of grid lines with the particles or grain surfaces and  $L$  is the total length of grid lines. Thus

$$f_V = f_A - \frac{Nl}{2L}$$

or

$$f_V = f_A - \frac{lt}{\pi A}. \quad (2)$$

It should be pointed out that in the measurement of  $S$  there will again exist an effect analogous to the Holmes effect in that the perimeter, or the number of intersections will appear to be larger than they actually are. This is a second order correction, however, which may also be easily estimated.

#### ACKNOWLEDGMENT

The author wishes to thank J. E. Hilliard for calling his attention to the Holmes effect.

#### REFERENCES

1. FELIX CHAYES, *Petrographic Modal Analysis*, Chap. 11, John Wiley and Sons, New York (1956).
2. JOHN W. CAHN AND JACK NUTTING, *J. Metals* (June, 1959).
3. V. VOUK (1948), *Nature*, **162**, 330.
4. C. S. SMITH AND L. GUTTMAN (1953), *Trans. A.I.M.E.*, **197**, 81-87.

THE AMERICAN MINERALOGIST, VOL. 44, MARCH-APRIL, 1959

#### GRAPHICAL REPRESENTATION OF AMPHIBOLE COMPOSITIONS\*

J. V. SMITH, *The Pennsylvania State University,*  
*University Park, Pennsylvania.*

Compositional variations of amphiboles are complex and difficult to memorize. As data are generally more easy to assimilate in a visual than in a mathematical form, a graphical representation is desirable.

Amphiboles fall readily into two groups,

*anthophyllite and cummingtonite* formula  $A_2B_5C_8O_{22}D_2$

where

A is largely Mg, Fe<sup>2+</sup>  
B is Mg, Fe<sup>2+</sup>, Al, Fe<sup>3+</sup> etc.  
C is Si, Al  
D is OH, F, Cl.

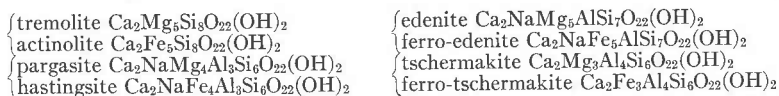
\* Contribution No. 58-21, College of Mineral Industries, Pennsylvania State University, University Park, Pennsylvania.

calcium-sodium amphiboles formula  $E_2$  to  ${}_3B_5C_8O_{22}D_2$ 

where E is Ca, Na, K etc.

In the first group the two important substitutions are Mg for  $Fe^2$  and 2Al for Si+(Mg,  $Fe^2$ ). Consequently this group of amphiboles can be graphically displayed on a square diagram with corners  $Mg_7Si_8O_{22}(OH)_2$ ,  $Fe_7Si_8O_{22}(OH)_2$ ,  $Mg_5Al_2Si_6Al_2O_{22}(OH)_2$ ,  $Fe_5Al_2Si_6Al_2O_{22}(OH)_2$  as is already well known (Winchell and Winchell, 1951).

In the second group, compositional variations are more complex, for there is interaction between ions of four different valencies. Sundius (1946) has determined a complete list of end members and his results and nomenclature will be adopted here. Hallimond (1943) has devised a graphical representation for calcic amphiboles with Ca=2. The diagram consists of a quadrilateral (Fig. 1) with apices



In this diagram Mg and Fe are included together; by erecting a vertical ordinate on this base the variation between the Mg and Fe and members can be shown, as, for example, in Winchell and Winchell (1951).

If, instead, a vertical ordinate is used that expresses the variation  $CaAl \rightarrow NaSi$ , the relationship between calcium and sodium amphiboles

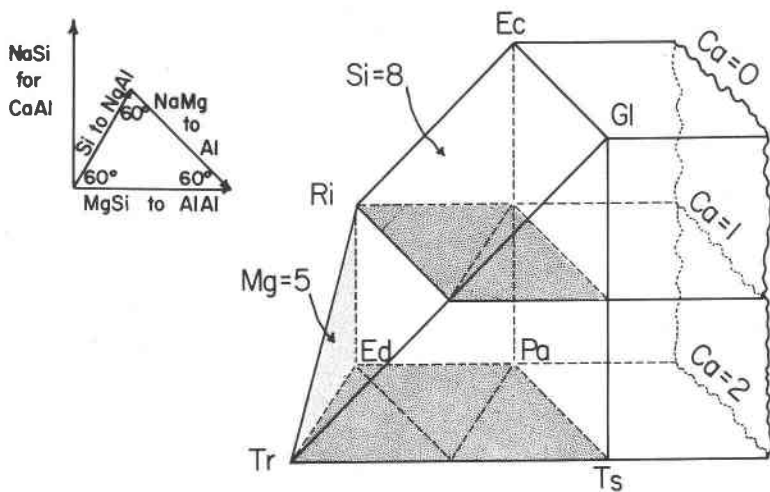


FIG. 1. Three-dimensional diagram showing the compositional variation in amphiboles. Tr, tremolite; Ts, tschermakite; Ed, edenite; Pa, pargasite; Ri, richterite; Ec, eckermanite; Gl, glaucophane. The inset diagram shows the atomic substitutions that form the basis of the large diagram.

can be readily seen (Fig. 1). When all the Ca has been exchanged for Na, pargasite (hastingsite) and tschermakite (ferro-tschermakite) are transformed into eckermannite  $\text{Na}_3\text{Mg}_4\text{AlSi}_8\text{O}_{22}(\text{OH})_2$  (arfvedsonite  $\text{Na}_3\text{Fe}_4\text{AlSi}_8\text{O}_{22}(\text{OH})_2$ ) and glaucophane  $\text{Na}_2\text{Mg}_3\text{Al}_2\text{Si}_8\text{O}_{22}(\text{OH})_2$  (riebeckite  $\text{Na}_2\text{Fe}_3\text{Al}_2\text{Si}_8\text{O}_{22}(\text{OH})_2$ ). When only one Ca has been exchanged edenite (ferro-edenite) is turned into richterite  $\text{CaNa}_2\text{Mg}_5\text{Si}_8\text{O}_{22}(\text{OH})_2$  (ferro-richterite  $\text{CaNa}_2\text{Fe}_5\text{Si}_8\text{O}_{22}(\text{OH})_2$ ).

The possible compositional variations of calcium-sodium amphiboles can be deduced from a crystal-chemical study of the amphibole structure, and readily visualized from the diagram. The upper limit of the diagram is simply fixed by the requirement that Ca does not fall below zero. Only rarely in published analyses is Ca greater than 2, and perhaps these exceptions are caused by analytical error. This fixes the lower limit of the diagram. The third limiting factor is that Si cannot be greater than 8 as only eight sites of tetrahedral coordination exist in the amphibole structure. In the diagram the plane with  $\text{Si} = 8$  passes through eckermannite, glaucophane, tremolite and richterite. All compositions to the left of this would have Si greater than 8 and therefore are forbidden. The fourth factor is that  $\text{Ca} + \text{Na}$  cannot be greater than 3, the number of large holes in the structure. Thus all compositions behind the plane defined by edenite, richterite, eckermannite and pargasite are forbidden. Fifthly, the sum of  $\text{Ca} + \text{Na}$  does not fall below 2 except in a few analyses, the structural reason apparently being that the large holes occupied in anthophyllite must be completely filled in all amphiboles. All compositions in front of the plane tremolite, glaucophane and tschermakite are therefore prohibited. The  $\text{Mg} + \text{Fe}^{2+}$  content provides the sixth criterion, for only 5 sites in the structure are available for these ions. Consequently all compositions to the left of the plane tremolite, edenite and richterite are forbidden. The final criterion is a practical one. Compositions to the right of the plane defined by pargasite, tschermakite, glaucophane and eckermannite rarely occur, which means that the substitution of Al in the amphibole structure is limited to considerably less than the theoretical maximum. Thus the compositional variation of hornblendes is limited to a wedge-shaped region with one corner cut off.

Difficulties arise when actual analyses are plotted on the diagram. For each of the four valence states, planes can be erected which express the amounts of the ions. Ideally the four planes should meet in a point but in practice discrepancies occur, some of them very large. The reasons for these have not yet been fully evaluated, although four can be readily suggested; error in the chemical analysis together with impurity in the analyzed material, occurrence of Mg and Fe in the large holes normally occupied by Na and Ca (equivalent to solid solution between a horn-

blende and the anthophyllite-cummingtonite series); replacement of  $\text{OH}^-$  by  $\text{O}^{2-}$  (the oxy-hornblende reaction) or the presence of an atomic substitution not considered in Sundius's scheme. The relative significance of these possibilities together with a way of recognizing them will be considered in a later publication. The diagram is presented at this time because of the hope that it will prove of help (especially to students) in visualizing the broad compositional variations of amphiboles.

The assistance obtained from a National Science Foundation grant is gratefully acknowledged.

#### REFERENCES

- SUNDIUS, N. (1946), *Sveriges Geologiska Undersökning Årsbok*, 40, number 4.  
WINCHELL, A. N., AND WINCHELL, H. (1951). *Elements of Optical Mineralogy*, Pt. 2, John Wiley and Sons, Inc.  
HALLIMOND, A. F. (1943), *Am. Mineral.*, 28, 65.

THE AMERICAN MINERALOGIST, VOL. 44, MARCH-APRIL, 1959

#### THE NEAR INFRARED SPECTRUM OF BERYL

KENNETH A. WICKERSHEIM AND ROBERT A. BUCHANAN, *University of California, Los Angeles, California.*

Several references to the Raman and infrared absorption bands of beryl in the 2.7 micron ( $3700 \text{ cm.}^{-1}$ ) region have appeared in the literature during the past twenty-six years. Nisi (1) observed a Raman band at  $3607 \text{ cm.}^{-1}$  using as a sample a clear, light green, hexagonal prism of beryl. No attempt was made to account for this frequency. Later Matossi and Bronder (2) reported the infrared spectrum of a sample of aquamarine taken with an instrument of low resolving power. Two strong bands were observed near  $3600$  and  $3700 \text{ cm.}^{-1}$ . In addition weaker clusters of bands were observed in the  $5000$  and  $7000 \text{ cm.}^{-1}$  regions. Matossi and Bronder felt that these bands were too intense to be due to a water impurity in the beryl, arguing that a 1 per cent impurity would be possible, but that the intensity of the bands would indicate a 5 to 10 per cent impurity. They suggested that the bands could be due to a hydroxyl impurity and to multiple combinations of silicate frequencies.

Lyon and Kinsey (3) studied a narrow region of the spectrum in the vicinity of  $3700 \text{ cm.}^{-1}$  under higher resolution using a grating spectrometer and a sample of beryl 0.2 mm. thick. They found two intense bands whose centers were estimated to be  $3598$  and  $3690 \text{ cm.}^{-1}$  plus a weak shoulder on the high frequency side of the second band. They identified these bands with envelopes of certain rotation branches of the sym-